EUROPEAN ORGANIZATION FOR NUCLEAR RESEARCH

CERN–EP/2000-134

31 October 2000

Search for sleptons in e^+e^- collisions at $\sqrt{s}$ =183 to 189 GeV

DELPHI Collaboration

Abstract

Data taken by the DELPHI experiment at centre-of-mass energies of 183 GeV and 189 GeV with a total integrated luminosity of 212 pb^{-1} have been used to search for the supersymmetric partners of the electrons, muons, and taus in the context of the Minimal Supersymmetric Standard Model (MSSM). The decay topologies searched for were the direct decay ($\tilde{\ell} \rightarrow \ell\tilde{\chi}_1^0$), producing acoplanar lepton pairs plus missing energy, and the cascade decay ($\tilde{\ell} \rightarrow \ell\tilde{\chi}_2^0 \rightarrow \ell\gamma\tilde{\chi}_1^0$), producing acoplanar lepton and photon pairs plus missing energy. The observed number of events is in agreement with Standard Model predictions. The 95% CL excluded mass limits for selectrons, smuons and staus are $m_{\tilde{e}} \leq 87$ GeV/c^2 , $m_{\tilde{\mu}} \leq 80$ GeV/c^2 and $m_{\tilde{\tau}} \leq 75$ GeV/c^2, respectively, for values of μ=-200 GeV/c^2 and tanβ=1.5.

(Euro. Phys. J. C19(2001)29)

P.Abreu[22], W.Adam[52], T.Adye[38], P.Adzic[12], I.Ajinenko[44], Z.Albrecht[18], T.Alderweireld[2], G.D.Alekseev[17], R.Alemany[9], T.Allmendinger[18], P.P.Allport[23], S.Almehed[25], U.Amaldi[29], N.Amapane[47], S.Amato[49], E.G.Anassontzis[3], P.Andersson[46], A.Andreazza[28], S.Andringa[22], N.Anjos[22], P.Antilogus[26], W-D.Apel[18], Y.Arnoud[15], B.Åsman[46], J-E.Augustin[24], A.Augustinus[9], P.Baillon[9], A.Ballestrero[47], P.Bambade[9,20], F.Barao[22], G.Barbiellini[48], R.Barbier[26], D.Y.Bardin[17], G.Barker[18], A.Baroncelli[40], M.Battaglia[16], M.Baubillier[24], K-H.Becks[54], M.Begalli[6], A.Behrmann[54], Yu.Belokopytov[9], N.C.Benekos[33], A.C.Benvenuti[5], C.Berat[15], M.Berggren[24], L.Berntzon[46], D.Bertrand[2], M.Besancon[41], N.Besson[41], M.S.Bilenky[17], M-A.Bizouard[20], D.Bloch[10], H.M.Blom[32], L.Bol[18], M.Bonesini[29], M.Boonekamp[41], P.S.L.Booth[23], G.Borisov[20], C.Bosio[43], O.Botner[50], E.Boudinov[32], B.Bouquet[20], C.Bourdarios[20], T.J.V.Bowcock[23], I.Boyko[17], I.Bozovic[12], M.Bozzo[14], M.Bracko[45], P.Branchini[40], R.A.Brenner[50], P.Bruckman[9], J-M.Brunet[8], L.Bugge[34], P.Buschmann[54], M.Caccia[28], M.Calvi[29], T.Camporesi[9], V.Canale[39], F.Carena[9], L.Carroll[23], C.Caso[14], M.V.Castillo Gimenez[51], A.Cattai[9], F.R.Cavallo[5], Ph.Charpentier[9], P.Checchia[37], G.A.Chelkov[17], R.Chierici[47], P.Chliapnikov[9,44], P.Chochula[7], V.Chorowicz[26], J.Chudoba[31], K.Cieslik[19], P.Collins[9], R.Contri[14], E.Cortina[51], G.Cosme[20], F.Cossutti[9], M.Costa[51], H.B.Crawley[1], D.Crennell[38], J.Croix[10], G.Crosetti[14], J.Cuevas Maestro[35], S.Czellar[16], J.D'Hondt[2], J.Dalmau[46], M.Davenport[9], W.Da Silva[24], G.Della Ricca[48], P.Delpierre[27], N.Demaria[47], A.De Angelis[48], W.De Boer[18], C.De Clercq[2], B.De Lotto[48], A.De Min[9], L.De Paula[49], H.Dijkstra[9], L.Di Ciaccio[39], K.Doroba[53], M.Dracos[10], J.Drees[54], M.Dris[33], G.Eigen[4], T.Ekelof[50], M.Ellert[50], M.Elsing[9], J-P.Engel[10], M.Espirito Santo[9], G.Fanourakis[12], D.Fassouliotis[12], M.Feindt[18], J.Fernandez[42], A.Ferrer[51], E.Ferrer-Ribas[20], F.Ferro[14], A.Firestone[1], U.Flagmeyer[54], H.Foeth[9], E.Fokitis[33], F.Fontanelli[14], B.Franek[38], A.G.Frodesen[4], R.Fruhwirth[52], F.Fulda-Quenzer[20], J.Fuster[51], A.Galloni[23], D.Gamba[47], S.Gamblin[20], M.Gandelman[49], C.Garcia[51], C.Gaspar[9], M.Gaspar[49], U.Gasparini[37], Ph.Gavillet[9], E.N.Gazis[33], D.Gele[10], T.Geralis[12], L.Gerdyukov[44], N.Ghodbane[26], I.Gil[51], F.Glege[54], R.Gokieli[9,53], B.Golob[9,45], G.Gomez-Ceballos[42], P.Goncalves[22], I.Gonzalez Caballero[42], G.Gopal[38], L.Gorn[1], Yu.Gouz[44], V.Gracco[14], J.Grahl[1], E.Graziani[40], G.Grosdidier[20], K.Grzelak[53], J.Guy[38], C.Haag[18], F.Hahn[9], S.Hahn[54], S.Haider[9], A.Hallgren[50], K.Hamacher[54], J.Hansen[34], F.J.Harris[36], S.Haug[34], F.Hauler[18], V.Hedberg[9,25], S.Heising[18], J.J.Hernandez[51], P.Herquet[2], H.Herr[9], O.Hertz[18], E.Higon[51], S-O.Holmgren[46], P.J.Holt[36], S.Hoorelbeke[2], M.Houlden[23], J.Hrubec[52], G.J.Hughes[23], K.Hultqvist[9,46], J.N.Jackson[23], R.Jacobsson[9], P.Jalocha[19], Ch.Jarlskog[25], G.Jarlskog[25], P.Jarry[41], B.Jean-Marie[20], D.Jeans[36], E.K.Johansson[46], P.Jonsson[26], C.Joram[9], P.Juillot[10], L.Jungermann[18], F.Kapusta[24], K.Karafasoulis[12], S.Katsanevas[26], E.C.Katsoufis[33], R.Keranen[18], G.Kernel[45], B.P.Kersevan[45], Yu.Khokhlov[44], B.A.Khomenko[17], N.N.Khovanski[17], A.Kiiskinen[16], B.King[23], A.Kinvig[23], N.J.Kjaer[9], O.Klapp[54], P.Kluit[32], P.Kokkinias[12], V.Kostioukhine[44], C.Kourkoumelis[3], O.Kouznetsov[17], M.Krammer[52], E.Kriznic[45], Z.Krumstein[17], P.Kubinec[7], M.Kucharczyk[19], J.Kurowska[53], J.W.Lamsa[1], J-P.Laugier[41], G.Leder[52], F.Ledroit[15], L.Leinonen[46], A.Leisos[12], R.Leitner[31], G.Lenzen[54], V.Lepeltier[20], T.Lesiak[19], M.Lethuillier[26], J.Libby[36], W.Liebig[54], D.Liko[9], A.Lipniacka[46], I.Lippi[37], J.G.Loken[36], J.H.Lopes[49], J.M.Lopez[42], R.Lopez-Fernandez[15], D.Loukas[12], P.Lutz[41], L.Lyons[36], J.MacNaughton[52], J.R.Mahon[6], A.Maio[22], A.Malek[54], S.Maltezos[33], V.Malychev[17], F.Mandl[52], J.Marco[42], R.Marco[42], B.Marechal[49], M.Margoni[37], J-C.Marin[9], C.Mariotti[9], A.Markou[12], C.Martinez-Rivero[9], S.Marti i Garcia[9], J.Masik[13], N.Mastroyiannopoulos[12], F.Matorras[42], C.Matteuzzi[29], G.Matthiae[39], F.Mazzucato[37], M.Mazzucato[37], M.Mc Cubbin[23], R.Mc Kay[1], R.Mc Nulty[23], G.Mc Pherson[23], E.Merle[15], C.Meroni[28], W.T.Meyer[1], E.Migliore[9], L.Mirabito[26], W.A.Mitaroff[52], U.Mjoernmark[25], T.Moa[46], M.Moch[18], K.Moenig[9,11], M.R.Monge[14], J.Montenegro[32], D.Moraes[49], P.Morettini[14], G.Morton[36], U.Mueller[54], K.Muenich[54], M.Mulders[32], L.M.Mundim[6], W.J.Murray[38], B.Muryn[19], G.Myatt[36], T.Myklebust[34], M.Nassiakou[12], F.L.Navarria[5], K.Nawrocki[53], P.Negri[29], S.Nemecek[13], N.Neufeld[52], R.Nicolaidou[41], P.Niezurawski[53], M.Nikolenko[10,17], V.Nomokonov[16], A.Nygren[25], V.Obraztsov[44], A.G.Olshevski[17], A.Onofre[22], R.Orava[16], K.Osterberg[9], A.Ouraou[41], A.Oyanguren[51], M.Paganoni[29], S.Paiano[5], R.Pain[24], R.Paiva[22], J.Palacios[36], H.Palka[19], Th.D.Papadopoulou[33], L.Pape[9], C.Parkes[9], F.Parodi[14], U.Parzefall[23], A.Passeri[40], O.Passon[54], T.Pavel[25], M.Pegoraro[37], L.Peralta[22], V.Perepelitsa[51], M.Pernicka[52], A.Perrotta[5], C.Petridou[48], A.Petrolini[14], H.T.Phillips[38], F.Pierre[41], M.Pimenta[22], E.Piotto[28], T.Podobnik[45], V.Poireau[41], M.E.Pol[6], G.Polok[19], P.Poropat[48], V.Pozdniakov[17], P.Privitera[39], N.Pukhaeva[17], A.Pullia[29], D.Radojicic[36], S.Ragazzi[29], H.Rahmani[33], P.N.Ratoff[21], A.L.Read[34], P.Rebecchi[9], N.G.Redaelli[29], M.Regler[52], J.Rehn[18], D.Reid[32], R.Reinhardt[54], P.B.Renton[36], L.K.Resvanis[3], F.Richard[20], J.Ridky[13], G.Rinaudo[47], I.Ripp-Baudot[10], A.Romero[47], P.Ronchese[37], E.I.Rosenberg[1], P.Rosinsky[7], T.Rovelli[5], V.Ruhlmann-Kleider[41], A.Ruiz[42], H.Saarikko[16], Y.Sacquin[41], A.Sadovsky[17], G.Sajot[15], L.Salmi[16], J.Salt[51], D.Sampsonidis[12], M.Sannino[14], A.Savoy-Navarro[24], C.Schwanda[52], Ph.Schwemling[24], B.Schwering[54], U.Schwickerath[18], F.Scuri[48], P.Seager[21], Y.Sedykh[17], A.M.Segar[36], R.Sekulin[38], G.Sette[14], R.C.Shellard[6], M.Siebel[54], L.Simard[41], F.Simonetto[37], A.N.Sisakian[17], G.Smadja[26], N.Smirnov[44], O.Smirnova[25], G.R.Smith[38], A.Sokolov[44], O.Solovianov[44], A.Sopczak[18], R.Sosnowski[53], T.Spassov[9], E.Spiriti[40], S.Squarcia[14], C.Stanescu[40], M.Stanitzki[18], K.Stevenson[36], A.Stocchi[20], J.Strauss[52], R.Strub[10], B.Stugu[4], M.Szczekowski[53], M.Szeptycka[53], T.Tabarelli[29], A.Taffard[23], F.Tegenfeldt[50], F.Terranova[29], J.Timmermans[32], N.Tinti[5], L.G.Tkatchev[17], M.Tobin[23], S.Todorova[9], B.Tome[22], A.Tonazzo[9], L.Tortora[40], P.Tortosa[51], D.Treille[9], G.Tristram[8], M.Trochimczuk[53], C.Troncon[28], M-L.Turluer[41], I.A.Tyapkin[17], P.Tyapkin[25], S.Tzamarias[12], O.Ullaland[9], V.Uvarov[44], G.Valenti[9,5], E.Vallazza[48], C.Vander Velde[2], P.Van Dam[32], W.Van den Boeck[2], J.Van Eldik[9,32], A.Van Lysebetten[2], N.van Remortel[2], I.Van Vulpen[32], G.Vegni[28], L.Ventura[37], W.Venus[38,9], F.Verbeure[2], P.Verdier[26], M.Verlato[37],

L.S.Vertogradov[17], V.Verzi[28], D.Vilanova[41], L.Vitale[48], E.Vlasov[44], A.S.Vodopyanov[17], G.Voulgaris[3], V.Vrba[13], H.Wahlen[54], A.J.Washbrook[23], C.Weiser[9], D.Wicke[9], J.H.Wickens[2], G.R.Wilkinson[36], M.Winter[10], M.Witek[19], G.Wolf[9], J.Yi[1], O.Yushchenko[44], A.Zalewska[19], P.Zalewski[53], D.Zavrtanik[45], E.Zevgolatakos[12], N.I.Zimin[17,25], A.Zintchenko[17], Ph.Zoller[10], G.Zumerle[37], M.Zupan[12]

[1]Department of Physics and Astronomy, Iowa State University, Ames IA 50011-3160, USA
[2]Physics Department, Univ. Instelling Antwerpen, Universiteitsplein 1, B-2610 Antwerpen, Belgium
and IIHE, ULB-VUB, Pleinlaan 2, B-1050 Brussels, Belgium
and Faculté des Sciences, Univ. de l'Etat Mons, Av. Maistriau 19, B-7000 Mons, Belgium
[3]Physics Laboratory, University of Athens, Solonos Str. 104, GR-10680 Athens, Greece
[4]Department of Physics, University of Bergen, Allégaten 55, NO-5007 Bergen, Norway
[5]Dipartimento di Fisica, Università di Bologna and INFN, Via Irnerio 46, IT-40126 Bologna, Italy
[6]Centro Brasileiro de Pesquisas Físicas, rua Xavier Sigaud 150, BR-22290 Rio de Janeiro, Brazil
and Depto. de Física, Pont. Univ. Católica, C.P. 38071 BR-22453 Rio de Janeiro, Brazil
and Inst. de Física, Univ. Estadual do Rio de Janeiro, rua São Francisco Xavier 524, Rio de Janeiro, Brazil
[7]Comenius University, Faculty of Mathematics and Physics, Mlynska Dolina, SK-84215 Bratislava, Slovakia
[8]Collège de France, Lab. de Physique Corpusculaire, IN2P3-CNRS, FR-75231 Paris Cedex 05, France
[9]CERN, CH-1211 Geneva 23, Switzerland
[10]Institut de Recherches Subatomiques, IN2P3 - CNRS/ULP - BP20, FR-67037 Strasbourg Cedex, France
[11]Now at DESY-Zeuthen, Platanenallee 6, D-15735 Zeuthen, Germany
[12]Institute of Nuclear Physics, N.C.S.R. Demokritos, P.O. Box 60228, GR-15310 Athens, Greece
[13]FZU, Inst. of Phys. of the C.A.S. High Energy Physics Division, Na Slovance 2, CZ-180 40, Praha 8, Czech Republic
[14]Dipartimento di Fisica, Università di Genova and INFN, Via Dodecaneso 33, IT-16146 Genova, Italy
[15]Institut des Sciences Nucléaires, IN2P3-CNRS, Université de Grenoble 1, FR-38026 Grenoble Cedex, France
[16]Helsinki Institute of Physics, HIP, P.O. Box 9, FI-00014 Helsinki, Finland
[17]Joint Institute for Nuclear Research, Dubna, Head Post Office, P.O. Box 79, RU-101 000 Moscow, Russian Federation
[18]Institut für Experimentelle Kernphysik, Universität Karlsruhe, Postfach 6980, DE-76128 Karlsruhe, Germany
[19]Institute of Nuclear Physics and University of Mining and Metalurgy, Ul. Kawiory 26a, PL-30055 Krakow, Poland
[20]Université de Paris-Sud, Lab. de l'Accélérateur Linéaire, IN2P3-CNRS, Bât. 200, FR-91405 Orsay Cedex, France
[21]School of Physics and Chemistry, University of Lancaster, Lancaster LA1 4YB, UK
[22]LIP, IST, FCUL - Av. Elias Garcia, 14-1^{o}, PT-1000 Lisboa Codex, Portugal
[23]Department of Physics, University of Liverpool, P.O. Box 147, Liverpool L69 3BX, UK
[24]LPNHE, IN2P3-CNRS, Univ. Paris VI et VII, Tour 33 (RdC), 4 place Jussieu, FR-75252 Paris Cedex 05, France
[25]Department of Physics, University of Lund, Sölvegatan 14, SE-223 63 Lund, Sweden
[26]Université Claude Bernard de Lyon, IPNL, IN2P3-CNRS, FR-69622 Villeurbanne Cedex, France
[27]Univ. d'Aix - Marseille II - CPP, IN2P3-CNRS, FR-13288 Marseille Cedex 09, France
[28]Dipartimento di Fisica, Università di Milano and INFN-MILANO, Via Celoria 16, IT-20133 Milan, Italy
[29]Dipartimento di Fisica, Univ. di Milano-Bicocca and INFN-MILANO, Piazza delle Scienze 2, IT-20126 Milan, Italy
[30]Niels Bohr Institute, Blegdamsvej 17, DK-2100 Copenhagen Ø, Denmark
[31]IPNP of MFF, Charles Univ., Areal MFF, V Holesovickach 2, CZ-180 00, Praha 8, Czech Republic
[32]NIKHEF, Postbus 41882, NL-1009 DB Amsterdam, The Netherlands
[33]National Technical University, Physics Department, Zografou Campus, GR-15773 Athens, Greece
[34]Physics Department, University of Oslo, Blindern, NO-1000 Oslo 3, Norway
[35]Dpto. Fisica, Univ. Oviedo, Avda. Calvo Sotelo s/n, ES-33007 Oviedo, Spain
[36]Department of Physics, University of Oxford, Keble Road, Oxford OX1 3RH, UK
[37]Dipartimento di Fisica, Università di Padova and INFN, Via Marzolo 8, IT-35131 Padua, Italy
[38]Rutherford Appleton Laboratory, Chilton, Didcot OX11 OQX, UK
[39]Dipartimento di Fisica, Università di Roma II and INFN, Tor Vergata, IT-00173 Rome, Italy
[40]Dipartimento di Fisica, Università di Roma III and INFN, Via della Vasca Navale 84, IT-00146 Rome, Italy
[41]DAPNIA/Service de Physique des Particules, CEA-Saclay, FR-91191 Gif-sur-Yvette Cedex, France
[42]Instituto de Fisica de Cantabria (CSIC-UC), Avda. los Castros s/n, ES-39006 Santander, Spain
[43]Dipartimento di Fisica, Università degli Studi di Roma La Sapienza, Piazzale Aldo Moro 2, IT-00185 Rome, Italy
[44]Inst. for High Energy Physics, Serpukov P.O. Box 35, Protvino, (Moscow Region), Russian Federation
[45]J. Stefan Institute, Jamova 39, SI-1000 Ljubljana, Slovenia and Laboratory for Astroparticle Physics,
Nova Gorica Polytechnic, Kostanjeviska 16a, SI-5000 Nova Gorica, Slovenia,
and Department of Physics, University of Ljubljana, SI-1000 Ljubljana, Slovenia
[46]Fysikum, Stockholm University, Box 6730, SE-113 85 Stockholm, Sweden
[47]Dipartimento di Fisica Sperimentale, Università di Torino and INFN, Via P. Giuria 1, IT-10125 Turin, Italy
[48]Dipartimento di Fisica, Università di Trieste and INFN, Via A. Valerio 2, IT-34127 Trieste, Italy
and Istituto di Fisica, Università di Udine, IT-33100 Udine, Italy
[49]Univ. Federal do Rio de Janeiro, C.P. 68528 Cidade Univ., Ilha do Fundão BR-21945-970 Rio de Janeiro, Brazil
[50]Department of Radiation Sciences, University of Uppsala, P.O. Box 535, SE-751 21 Uppsala, Sweden
[51]IFIC, Valencia-CSIC, and D.F.A.M.N., U. de Valencia, Avda. Dr. Moliner 50, ES-46100 Burjassot (Valencia), Spain
[52]Institut für Hochenergiephysik, Österr. Akad. d. Wissensch., Nikolsdorfergasse 18, AT-1050 Vienna, Austria
[53]Inst. Nuclear Studies and University of Warsaw, Ul. Hoza 69, PL-00681 Warsaw, Poland
[54]Fachbereich Physik, University of Wuppertal, Postfach 100 127, DE-42097 Wuppertal, Germany

1 Introduction

During the 1997 and 1998 data taking period, the LEP accelerator operated at centre-of-mass energies of 183 GeV and 189 GeV respectively. This allowed an extension of the searches for scalar partners of electrons, muons, and taus, predicted by supersymmetric models, over the limits on the production of these particles obtained from data previously taken at centre-of-mass energies of 130-172 GeV [1]. This paper reports on a search for these particles using the 212 pb^{-1} of data taken by DELPHI during 1997 and 1998. Similar searches have been performed by other collaborations [2].

For a realistic experimental search one has to make some well motivated assumptions. In this analysis, the model assumed is the Minimal Supersymmetric Standard Model (MSSM) [3]. In the case that the MSSM is locally invariant (often referred to as *minimal supergravity*), the number of free parameters set at the unification scale (the scale at which gauge couplings unify) can be reduced to five[1]:

$$\tilde{m}_0, \quad \tilde{m}_{1/2}, \quad A, \quad B, \quad \mu .$$

These are respectively, the universal scalar and gaugino masses, the universal trilinear and bilinear[2] scalar couplings, and the Higgs doublets mass mixing parameter.

In this analysis R-parity[3] conservation is also assumed, which leads to three important phenomenological consequences [5]. Firstly, the *lightest supersymmetric particle* (LSP) must be absolutely stable. If the LSP is electrically neutral, as favoured by cosmological constraints, it interacts only weakly with ordinary matter, so escaping detection. Secondly, each supersymmetric particle (sparticle) other than the LSP must eventually decay into a state which contains an odd number of LSPs, typically just one. Finally, R-parity conservation implies that collider experiments could only produce sparticles in even numbers.

Consequently, sleptons could be pair produced at LEP via $\mathrm{e}^+\mathrm{e}^-$ annihilation into Z^0/γ (Figure 1.a). In addition, selectrons can be produced from t-channel neutralino exchange, which introduces a direct dependence on the SUSY parameters and the possibility of left and right handed final states even without mixing via the mass matrix (Figure 1.b).

In a large fraction of the SUSY parameter space the dominant decay of the sleptons ($\tilde{\ell}$) is to the corresponding lepton flavour plus the lightest neutralino ($\tilde{\chi}_1^0$) (Figure 2.a), presumed from the MSSM mass spectrum to be the LSP. The neutralino will escape undetected, hence the topology will be characterised by acoplanar lepton pairs together with missing energy. In most of the analyses described in this paper we search specifically for such a signature.

The search can be extended by looking for topologies other than acoplanar lepton pairs. For certain values of SUSY parameters it is possible for the second lightest neutralino $\tilde{\chi}_2^0$ to be lighter than the sleptons. If this is the case the slepton can also decay via a cascade to a $\tilde{\chi}_1^0$, with a possible decay chain $\tilde{\ell} \to \ell\tilde{\chi}_2^0 \to \ell\gamma\tilde{\chi}_1^0$ (Figure 2.b). In order to investigate this channel we have searched DELPHI data for events containing acoplanar lepton and photon pairs plus missing energy.

[1] See [4] [5] [6] and references therein for further information on the actual supersymmetry breaking mechanism, and motivation for the assumptions made.

[2] Using renormalisation group evolution, the bilinear term is expressed in the low energy MSSM as $\tan\beta$, the ratio of the vacuum expectation values of the two Higgs doublets.

[3] R-parity is a quantum number, defined as R = $(-1)^{3(B-L)+2S}$ [5], with B, L, and S respectively the baryon number, the lepton number and the spin of the particle. Non-supersymmetric particles, including the Higgs scalars are R-*even*, whilst the supersymmetric particles are all R-*odd*.

2 Detector description

The DELPHI detector and its performance have been described in detail elsewhere [7] [8]; in the following we present only a brief description of the components relevant to the analyses presented here.

A system of cylindrical tracking chambers coupled with a 1.2 T uniform solenoidal magnetic field, directed along the beam axis, enables the reconstruction of charged particle tracks. The Vertex Detector (VD) consists of three cylindrical layers of silicon detectors, at radii 6.3 cm, 9.0 cm and 11.0 cm. The vertex tracking is aided in the forward regions by mini-strips and pixel detectors making up the Very Forward Tracker (VFT) [9] with an angular acceptance between 10° and 25°. The Inner Detector (ID) is a cylindrical drift chamber (inner radius 12 cm and outer radius 22 cm). The Time Projection Chamber (TPC), the principal tracking device of DELPHI, is a cylinder of 30 cm inner radius, 122 cm outer radius and a length of 2.7 m. Each end-plate is divided into 6 sectors, with 192 sense wires used for the dE/dx measurement and 16 circular pad rows used for 3 dimensional space-point reconstruction. The Outer Detector (OD) is composed of 24 planks each with 5 layers x 32 columns of drift tubes. The tubes, situated at radii between 196 cm and 207 cm from the beam axis, improve the precision of the momenta of the charged particles measured by the TPC. In addition to the barrel tracking, two planes of drift chambers, Forward Chambers A (FCA) and B (FCB), aligned perpendicular to the beam axis, allowed tracking in the endcap of the detector, giving a polar coverage down to 11° and 169° with respect to the e^- beam direction.

The electromagnetic calorimetery consists of the High density Projection Chamber (HPC), covering the barrel region of polar angle θ in the range $43° < \theta < 137°$, the Forward ElectroMagnetic Calorimeter (FEMC), consisting of 9064 Cherenkov lead glass blocks covering $11° < \theta < 36°$ and $144° < \theta < 169°$, and the STIC (Scintillator TIle Calorimeter), extending the coverage down to 1.66° from the beam axis in either direction. The 40° taggers are a series of single layer scintillator lead counters used to veto photons and electrons that would otherwise have been missed in the region between the HPC and FEMC.

The hadron calorimeter (HCAL) covers 98% of the solid angle. Muons with momenta above 2 GeV traverse the HCAL and are recorded in a set of muon drift chambers; the MUon Barrel (MUB) chambers, MUon Forward (MUF) chambers and the Surround Muon Chambers (SMC).

The identification of muons is provided primarily by the algorithm described in [8], which relies on the association of charged particles to signals in the barrel and forward muon chambers. In order to reduce contamination from cosmic ray particles, the impact parameter with respect to the beam crossing point was required to be less than 1.5 mm in the $R - \phi$ plane.

Electrons are identified as charged particle tracks with an energy deposit above 3 GeV in the electromagnetic calorimeter and with the ratio of the electromagnetic calorimeter energy to the track momentum from the track above $0.3c$. In addition, the shape of the shower profile in the HPC and the dE/dx measurement in the TPC were also considered. Forward electrons are distinguished from gamma conversions by requiring hits in the VFT.

A charged particle is identified as a pion if the energy deposited in the HCAL is greater than 2 GeV, greater than the energy deposited in the electromagnetic calorimeters and it does not produce hits in the muon chambers.

3 Data samples and event generators

The total integrated luminosity accumulated by the DELPHI experiment over the two years analysed was 212 pb^{-1}. This included 54 pb^{-1} of data collected at a centre-of-mass energy of 183 GeV and 158 pb^{-1} collected at 189 GeV.

Several programs were used to simulate Standard Model (SM) and SUSY (signal) events in order to estimate background contamination and signal efficiencies.

All the models used JETSET 7.4 [10] for quark fragmentation with parameters tuned to represent DELPHI data [11]. The program SUSYGEN [12] was used to generate slepton events and to calculate cross-sections and branching ratios. The generator EXCALIBUR [13] was used to model all four-fermion events, which includes the coherent interference of all diagrams leading to a given final state. For a cross check, PYTHIA [10] was used to generate samples of WW, ZZ, Weν and Zee events. The processes $e^+e^- \rightarrow Z^0/\gamma \rightarrow q\overline{q}(\gamma)$ were simulated by PYTHIA, whilst the two-fermion backgrounds $e^+e^- \rightarrow Z^0/\gamma \rightarrow \mu^+\mu^-(\gamma)$ and $\tau^+\tau^-(\gamma)$ events were produced by KORALZ [14]. The generators BABAMC [15] and BHWIDE [16] were used to simulate Bhabha scattering. Two-photon interactions leading to hadronic final states were simulated using TWOGAM [17] and BDKRC [18] for the Quark Parton Model contribution. BDK [19] was used for final states with electrons only, whilst final states with muons or taus were simulated using BDKRC.

Generated signal and background events were passed through a detailed detector response simulation (DELSIM) [8] and processed with the same reconstruction and analysis programs as the data. The number of background events simulated was several times larger than the number expected in the data.

4 Search for selectrons and smuons ($\tilde{\ell} \rightarrow \ell\widetilde{\chi}_1^0$)

The analysis was performed in two stages. Firstly a loose pre-selection was used to obtain a sample containing events with two oppositely charged tracks. At this stage, various distributions of the real data were compared with distributions from simulated SM events.

After this stage a tighter selection was applied. Tuned to both simulated background events and signal events, selections were made in order to reduce the expected SM background whilst keeping a reasonable efficiency for the signal over a wide range of the $\tilde{\ell}$–$\widetilde{\chi}_1^0$ mass combinations.

4.1 Search for selectrons

To search for selectrons, the general topology required was two acoplanar electrons and missing energy. The preliminary event selection kept all candidates with exactly two well reconstructed oppositely charged particles with momentum above 1 GeV/c. One of the two charged particles was required to be identified as an electron, rejecting events if the other was identified as a muon. At this stage in the analysis, the selection consisted mainly of Bhabha and two-photon events, with satisfactory agreement observed between data and simulated background (Figure 3).

To further reduce the SM backgrounds, tighter cuts were applied. As two-photon events are predominantly at low polar angles and with low momentum it was required that the visible energy be greater than 15 GeV and that the energy deposited in the low angle STIC calorimeter be less than 4 GeV. As a further constraint, the invariant mass

of the two tracks was required to be greater than 4.5 GeV/c^2, and the total transverse momentum with respect to the beam axis was required to be greater than 5 GeV/c.

To reduce the number of Bhabha events an upper limit on the visible energy of 100 GeV was imposed, whilst also requiring that the neutral energy not associated to the charged tracks be less than 30 GeV. Events were also rejected if there were more than four neutral clusters in total, each with energy above 0.5 GeV. Bhabha events are coplanar with a large opening angle, hence it was necessary that the acoplanarity and acolinearity be greater than 15°.

Four-fermion events were reduced by the constraints described above, in particular the constraint on the visible energy.

Contraints were also imposed on the momenta of the two tracks, requiring that both tracks had momenta above 2 GeV/c. It was further required that the missing momentum vector pointed to an active region of the detector.

The efficiency for the signal detection depends on the masses of $\tilde{\mathrm{e}}$ and $\tilde{\chi}^0_1$. The typical signal efficiency is ≈ 50 %.

After this selection a total of 56 candidates were found in the 212 pb^{-1} of data analysed, compared to 51.2 $\pm$ 1.5 predicted from SM processes. Details are given in Table 1.

4.2 Search for smuons

As a pre-selection, exactly two well reconstructed oppositely charged particles with momenta above 1 GeV/c were required. At least one of the particles had to be identified as a muon. It was further required that neither track be identified as an electron. The pre-selection sample consisted mainly of two-photon events, and good agreement between real data and simulated background was observed (Figure 4).

To further reduce SM backgrounds tighter cuts were applied. It was seen that using a sequential cut analysis, the dominant background after a tighter selection was W-pair events. These events become increasingly important in regions of high slepton mass and high Δm ($m_{\tilde{\mu}}$-$m_{\tilde{\chi}^0_1}$), where the signal events become virtually indistinguishable from the W-pair background. In these regions of SUSY mass space the cross-section for smuon production is low[4], and hence using sequential cuts to remove this background has a severe effect on the signal sensitivity.

Consequently for the 189 GeV data analysis, a different approach was adopted to the 183 GeV analysis, applying a selection procedure which depended on the ($\tilde{\mu}$, $\tilde{\chi}^0_1$) mass difference. For a mass difference, Δm, less than 35 GeV/c^2 where two-photon backgrounds are important, an analysis based on sequential cuts was performed. For the data taken at 183 GeV this approach was used for the full SUSY mass spectrum. However, in the 189 GeV analysis, for regions of Δm greater than 35 GeV/c^2, where the W-pair backgrounds are kinematically favoured, a probabilistic analysis based on the likelihood of an event being compatible with W-pair production was used.

For regions of Δm less than 35 GeV/c^2, to remove the two-photon events, the visible energy was required to be greater than 10 GeV. Also the energy in the STIC had to be less than 1 GeV. As a further constraint it was necessary for the invariant mass of the lepton pair to be greater than 4.5 GeV/c^2.

To remove $\mathrm{e^+e^-} \rightarrow \mathrm{Z^0}/\gamma \rightarrow \mu^+\mu^-$ events in this Δm region an upper limit on the visible energy of 120 GeV was imposed whilst also requiring the unassociated neutral energy to be less than 10 GeV, with no more than two neutral clusters. This background

[4] In the selectron scenario the t-channel contribution can enhance selectron production for low neutralino masses, hence increasing signal sensitivity in the mass regions dominated by W-pair backgrounds.

was further suppressed by accepting only events in which the opening angle between the tracks was less than 165° and the acoplanarity was greater than 15°.

To reduce W-pair contamination in this low Δm region, at a small cost in signal efficiency, events were rejected if the positively charged muon was within 40° of the e^+ beam direction, or the negatively charged muon was within 40° of the e^- beam direction.

For the selection of events kinematically allowed in regions of Δm greater than 35 GeV/c^2, a discriminating variable was constructed for the events in the 189 GeV data using the probability density functions (p.d.f's) of W-pair event variables after the pre-selection stage. The following variables were chosen due to their high discriminating power between signal and four-fermion events and their relatively low correlations:

- Product of lepton polar angle and charge (Q cosθ);
- Neutral energy;
- Opening angle between the leptons;
- Acoplanarity;
- Missing energy;
- Missing transverse momentum.

In addition, these variables have excellent agreement between real data and simulated background.

The discriminating function is shown in Figure 5 for data and simulated background (which is predominantly 2-photon at this stage). Also shown is the comparison of the discriminant variable for a sample of 4-fermion events and a sample of SUSY signal with a Δm value close to the W mass (80 GeV/c^2).

Two-photon and di-muon events were removed using the same cuts as in the low mass window. W-pair contamination was reduced by cutting on the discriminating function such that signal to background was maximised. It was further required that the missing momentum vector pointed towards active components of the DELPHI detector.

The efficiency for the signal detection depends on the masses of $\tilde{\mu}$ and $\widetilde{\chi}_1^0$. The cuts used to remove the SM background resulted in typical efficiencies of $\approx$ 50 % for the regions of low Δm, and $\approx$ 35 % for the regions of high Δm.

Table 2 summarises the number of accepted events in the data together with the predicted number of events from background sources. In the data collected at 189 GeV, for the regions of $\Delta m \leq$ 35 GeV/c^2, 17 candidates passed the tight selection, consistent with a background prediction of 17.5 $\pm$ 0.3 events. For the regions of $\Delta m >$ 35 GeV/c^2, 7 candidates remained compared with a background prediction of 9.2 $\pm$ 0.2 events. In the analysis of data taken at a centre-of-mass energy of 183 GeV, 5 candidates remained with an expectation of 6.1 $\pm$ 0.6 events from SM processes.

5 Search for staus

The off-diagonal terms of the slepton mass matrix are proportional to the mass of the corresponding SM partners. Important effects caused by these terms must be considered when searching for staus. For a certain mixing between right and left handed staus, the low-mass stau eigenstate ($\tilde{\tau}_1$) can become an important candidate for the lightest charged supersymmetric particle. Another consequence of the possible mixing of staus is the change of the coupling to the Z^0, and consequently the production cross-section, with the mixing angle.

5.1 Search for heavy staus

The characteristic signature of the production of pairs of heavy staus is the detection of a $\tau^+\tau^-$ pair with large acoplanarity and missing energy. Due to the scalar nature of the stau, the visible system will tend to be at large angles to the beam.

Among the SM background processes to this signal are s-channel production of tau pairs, in particular if they arise from a radiative return to the Z^0, with the ISR photon escaping detection, and four-fermion events where the final state contains two taus as the only visible particles. Finally, two photon interactions with $\gamma\gamma \to \tau^+\tau^-$ contribute in the case of staus close in mass to the LSP.

To select events with two taus, well reconstructed charged and neutral particles were first collected into clusters of total invariant mass below 5.5 GeV/c^2. Events with exactly two particle clusters (possibly accompanied by isolated neutral particles) were considered further if there were no more than 6 charged tracks in the event and these gave a total charge of 0 or $\pm$ 1. At least two tracks were required to have momentum above 1 GeV/c with one greater than 4 GeV/c. The distributions of data and simulated SM events agree well at this stage in the analysis, as can be seen in Figure 6.

To ensure that the selected events had the high acoplanarity typical for the signal, the acoplanarity angle was required to be above 10° (11° for the 183 GeV sample).

Selecting events at high angles to the beam was done by demanding that at least two charged particles with momentum above 1 GeV/c were observed above 30° to the beam axis. Also, the direction of the vectorial sum of momenta should be contained in the barrel region at an angle greater than 37° to the beam (30° in the 183 GeV sample). To reduce the background from radiative returns to the Z^0, none of the clusters were allowed to have a total momentum ($p^{\rm JET}$) above 67 GeV/c (60 GeV/c in the 183 GeV sample), the energy of isolated photons had to be below 20 GeV and there should be no signal in any 40° tagger. Furthermore, the value of the reduced centre-of-mass energy ($\sqrt{s'}$) was estimated using the angles of the jets, and assuming that a photon was lost in the beam-pipe (the triangle rule). This value should not fall in the interval 90 to 94 GeV (no such cut was made for the 183 GeV sample). In addition, there had to be no calorimetric energy below 30° in polar angle. This last cut was also very effective against the background from two-photon events, as it removed all such events where either of the initial e^+e^- were deflected into the forward calorimeters. The two-photon background was also reduced by discriminating against events where the two clusters were close together: the acoplanarity angle should not exceed 170° (176° for the 183 GeV sample).

In order to further suppress the background from $e^+e^- \to Z^0/\gamma \to \tau^+\tau^-$ events with τ-decays highly asymmetric in visible momentum, the square of the transverse momentum with respect to the thrust axis (δ) had to be above 0.9 (GeV/c)^2. This was the case for the 189 GeV sample; the condition was more complex in the 183 GeV sample (see below).

At this stage of the analysis, the background was dominated by the W-pair background, and in order to further suppress it, the events were analysed under the assumption that they were indeed W-pair events. The θ angle of the positive W (θ_{W^+}) was reconstructed by assuming that the direction of the taus was indentical to that of the jets and applying an unsmearing procedure (derived from simulated W-pair events) to estimate the true momentum of the taus. The final estimate of θ_{W^+} was then given by the average of the polar angle of the positive jet, the complement of the polar angle of the negative jet, and the two approximate solutions to the equation determining the W angle. As the signal is isotropic, whilst the W production is enhanced in the forward-backward direction and concentrated at high values of the higher of the two jet momenta ($p^{\rm JET}_{max}$), it was required that the observed values of θ_{W^+} (in radians) and $p^{\rm JET}_{max}$ (in GeV/c) were below the higher

of the two lines $\theta_{W^+} = 1.5$ and $\theta_{W^+} = -0.05\ p_{max}^{\rm JET} + 3.7$ in the $p_{max}^{\rm JET} - \theta_{W^+}$ plane. This cut was applied to the 189 GeV sample; in the 183 GeV sample, the simpler cut $\theta_{W^+} \leq 2.5$ radians was used.

This selection was supplemented by cuts that depended on the region of the ($m_{\tilde{\tau}}$,$m_{\tilde{\chi}_1^0}$) plane considered, which were tuned to remove the corresponding backgrounds for that region. The sub-division was different in the two samples, as were the cuts depending on the region. For the 189 GeV sample, two regions were defined: $\Delta m = m_{\tilde{\tau}}$-$m_{\tilde{\chi}_1^0}$ below or above 20 GeV/c^2. In the region of low mass difference, where the remaining two-photon background was concentrated, it was required that the missing transverse momentum ($p_T^{\rm miss}$) was greater than 5.4 GeV/c whilst, in the region of high Δm, the $p_T^{\rm miss}$ was required to be above 8 GeV/c. In the lower (higher) Δm region, it was also required that the highest momentum of any identified lepton in the event was less than 20 GeV/c (22 GeV/c), in order to further suppress the remaining W-pair background.

For the 183 GeV sample three regions of Δm were considered: less than 22 GeV/c^2 $22 - 50$ GeV/c^2 and more than 50 GeV/c^2. In these three regions, δ was required to exceed 0.4, 1.0 and 0.4 (GeV/c)^2 respectively, and $p_T^{\rm miss}$ to exceed 5.5, 6, and 6 GeV/c, respectively. The momentum of any identified lepton in the event should be less than 30 GeV/c (independent of Δm).

Table 3 summarises the number of accepted events in the data for the different selections together with the expected numbers of events from the different background channels. In the 212 pb^{-1} data sample analysed, 16 candidates were found, with a background estimation of 18.1 ± 0.8 from SM processes. The signal detection efficiency was of the order of 20% for the 189 GeV sample and 30% for the 183 GeV sample.

5.2 Search for light staus without coupling to the Z^o

To a large extent a light stau can be excluded using the agreement of the decay width of the Z^0 resonance with the SM prediction, as observed at LEP1 [20]. The corresponding cross-section limit of 150 pb for non-standard processes at $\sqrt{s} = M_{\rm Z}$ excludes a $\tilde{\tau}_R$ below 25 GeV/c^2. However, at the stau mixing angle giving the minimum cross-section, the coupling to the Z^0 vanishes and no exclusion is possible using this method. The high mass analysis described in the previous section loses its efficiency for stau masses below 20 GeV/c^2. This is mainly due to the fact that the stau-pairs are highly boosted at such a low mass, so that they fail the acoplanarity cut. Therefore a specific search was required for $m_{\tilde{\tau}}$ in the range from m_τ to 27 GeV/c^2 and this mixing angle. After selecting two tau events as described in the previous section, it was required that there was no identified isolated photon in the event. To reduce the background from Bhabha scattering, we demanded that the acolinearity angle was above 0.4° and $p_{max}^{\rm JET}$ below 70 GeV/c. Furthermore, the missing transverse momentum in the event was required to be above 6 GeV/c, the angle of the most energetic track in each hemisphere of the detector to be above 50° to the beam, and the direction of the vectorial sum of momenta should be above a polar angle of 40°. To further reduce the background from radiative return to the Z^0, the value of $\sqrt{s'}$ should not be between 82 to 102 GeV [5].

For $m_{\tilde{\tau}}$ above 15 GeV/c^2, the cut on acoplanarity was more restrictive: it was demanded to be above 4°.

With these cuts, a total of 122 events were selected in the mass region below 15 GeV/c^2 and 50 events in the higher region. The SM background was estimated to 150.1 ± 2.3 and 55.7 ± 1.7 in the two regions (Table 4). The efficiencies were practically flat for both mass

[5] It should be noted that as a consequence of the vanishing coupling to the Z^0, radiative return does not occur in $\tilde{\tau}$ production at the mixing angle yielding the minimal cross-section, even at $m_{\tilde{\tau}}$ below $M_Z/2$.

ranges. In the first case, the efficiency was around 25%, decreasing to 10% for $\Delta m = m_\tau$. In the second case it was around 15%, decreasing to ≤ 2 % for $\Delta m < 2\,\mathrm{GeV}/c^2$.

6 Search for cascade decays

In order to extend the slepton search, topologies from cascade decays of the $\tilde{\ell}$ have been considered. There are regions of the SUSY parameter space where the sleptons may also decay into the $\tilde{\chi}_2^0$ plus the corresponding lepton ($\tilde{\ell} \to \ell\tilde{\chi}_2^0$).

For smuons it presents some advantages as the dependence of the smuon mass limit on the SUSY parameter μ is considerably reduced. The $\tilde{\chi}_2^0$ may decay to $\tilde{\chi}_1^0\gamma$, with the $\tilde{\chi}_1^0$ being the LSP which escapes undetected. The topology for these events is acoplanar lepton pairs and two photons plus missing energy. The main advantage of searching for this type of event is that the experimental signature is very clean with very small SM backgrounds since the emission of photons requires higher orders and extra α_{EM} factors. However the cascade decay may be suppressed as the branching ratio $BR(\tilde{\chi}_2^0 \to \tilde{\chi}_1^0\gamma)$ may be small. The $BR(\tilde{\chi}_2^0 \to \tilde{\chi}_1^0\gamma)$ is close to 1 when both neutralinos have a similar mass, but in this near degenerate case the outgoing photon has low energy, so making detection difficult.

The search for these events was done in a two step procedure. First, samples of $ee\gamma\gamma$ and $\mu\mu\gamma\gamma$ events were selected following loose cuts. Before applying a tighter selection a likelihood function was defined for the main background channels (one for tagging Bhabha events in the $ee\gamma\gamma$ sample and the second one for tagging the $e^+e^- \to \mu^+\mu^-$ entering the $\mu\mu\gamma\gamma$ samples) contributing to the sample. Then the tight selection is combined with the likelihood in order to remove those events compatible with the SM processes.

6.1 $ee\gamma\gamma$ selection

A sample of $ee\gamma\gamma$ events was selected requiring only two charged tracks reconstructed with momentum greater than 3 GeV/c and at least two photons reconstructed with energy above 1 GeV. If several photons were selected, only the most energetic two were retained. Events were rejected if either of the charged tracks was consistent with positive pion or muon identification (see section 2). An acceptance cut demanding that all 4 particles should lie in the $10^\circ < \theta < 170^\circ$ region was applied in order to remove most of the two-photon interactions. The same cut was applied to the missing momentum vector, since this can be close to the beam axis for events coming from a radiative return to the Z^0. Finally the acolinearity of the electron and photon pairs had to be larger than 3°. After this stage in the analysis, reasonable agreement was observed between real data and simulated SM processes contributing to the sample (Figure 7).

The Bhabha likelihood was built according to the probability density functions (p.d.f's) of the visible energy, invariant mass between the electron-photon pair with smallest opening angle, the invariant mass of the electron pair and most energetic photon, and the angle between the missing momentum and the closest electron and photon.

A sample with most SM events removed was selected by demanding that the events satisfying the loose $ee\gamma\gamma$ selection comply with the following cuts: acolinearity and acoplanarity of the electron and photon pairs above 6° and a Bhabha probability less than 3%. According to this selection, 4.2 ± 0.9 events were expected from the SM and 5 seen (Table 5).

The efficiency for signal detection depended on the lepton and photon energies. An efficiency map was computed for a range of points of the SUSY parameter space. Typical efficiencies for detection were of the order of 40%.

6.2 $\mu\mu\gamma\gamma$ selection

The selection of a sample of $\mu\mu\gamma\gamma$ events proceeded in a similar manner to that of the $ee\gamma\gamma$ events. It was required that at least one of the charged tracks had to be identified as a muon, and neither of them as an electron. The rest of the kinematic cuts were the same as mentioned in the $ee\gamma\gamma$ selection. Events with more than two photons were further considered if the energy of the extra photon(s) was below 10 GeV.

The $e^+e^- \to \mu^+\mu^-$ likelihood was built from the p.d.f.s of the visible energy, momentum of the leading muon, invariant mass of the muon pair with the most energetic photon, the angle between the missing momentum and the closest muon, and the opening angle of the muon pair.

The tight $\mu\mu\gamma\gamma$ selection consisted basically of the same topological cuts as the tight $ee\gamma\gamma$ selection. In addition to these cuts, it was required that the likelihood for an event being consistent with $e^+e^- \to \mu^+\mu^-$ be less than 5%. With these cuts 2.9 ± 0.7 events were expected from the SM and 3 seen in the data (Table 6). The cuts used to remove SM background resulted in typical efficiencies for signal detection of 45%.

7 Results

Limits on slepton masses can be derived using several different assumptions. Scalar mass unification suggests lower masses and cross-sections for the partners of right handed fermions. Hence we have assumed that only right handed selectrons ($\tilde{\mathrm{e}}_R$) and smuons ($\tilde{\mu}_R$) are produced, leading to conservative mass limits.

For third generation sfermions, Yukawa couplings can be large, leading to an appreciable mixing between the pure weak hypercharge states. The production cross-section depends on this mixing, due to the variation in strength of the coupling to the Z^0 component of the weak current, and has a minimum at a mixing angle of 42°. Consequently, the results for the stau analyses are presented under these two assumptions; right handed stau production ($\tilde{\tau}_R$), and minimal mixing stau production ($\tilde{\tau}_{min}$).

8 Exclusion limits

Exclusion limits for slepton pair ($\tilde{\ell}\tilde{\ell}$) production were obtained, taking into account the signal efficiencies for each $\tilde{\ell} - \tilde{\chi}_1^0$ mass point, the cross-section and branching ratios for slepton production, and the number of data and background events kinematically compatible for a given mass combination. Signal events have been generated assuming model input values of $\tan\beta = 1.5$ and μ = -200 GeV/c^2. The limits were calculated using a likelihood ratio method described in [21]. Expected exclusion zones were calculated using the same algorithm, from simulated background-only experiments.

Figure 8.a shows the 95% CL exclusion regions for $\tilde{\mathrm{e}}_R\tilde{\mathrm{e}}_R$ production, obtained using the full 212 pb^{-1} of data. For the selectrons, we exclude masses up to $m_{\tilde{\mathrm{e}}_R} \leq 87$ GeV/c^2, providing the mass difference between the selectron and the LSP is above 20 GeV/c^2.

Figure 8.b shows the 95% CL exclusion regions for $\tilde{\mu}_R\tilde{\mu}_R$ production, obtained by combining the 183 GeV data with the 189 GeV data. For the smuons, we exclude masses up to $m_{\tilde{\mu}_R} \leq 80$ GeV/c^2, providing the mass difference between the smuon and the LSP is above 5 GeV/c^2.

Exclusion limits on $\tilde{\tau}\tilde{\tau}$ production were obtained taking into account the signal efficiencies for each $\tilde{\tau} - \tilde{\chi}_1^0$ mass point. When determining whether data or background events were kinematically compatible with the mass point, the end point of the expected momentum spectrum of the visible reconstructed tau was used. Figure 8.c shows the 95% CL $\tilde{\tau}_R$ exclusion region obtained by combining the previous data at lower energies with the 183 GeV and 189 GeV data, and Figure 8.d shows the exclusion regions in the case of the mixing angle yielding the minimal cross-section. For the staus, a mass limit can be set at 73 to 75 GeV/c^2 (depending on mixing) for mass differences between the stau and the LSP above 10 GeV/c^2. The dedicated search for a low-mass stau yields that a $\tilde{\tau}$ of a mass below 12.5 GeV/c^2 is excluded at 95% CL for any mixing angle, provided that Δm is greater than m_τ.

For the cascade decay analysis, assuming $\tilde{e}_R\tilde{e}_R$ or $\tilde{\mu}_R\tilde{\mu}_R$ production, one can set exclusion regions in the SUSY parameter space. To set limits, one has to consider the cross section for the selectron or smuon production and the branching ratios for the $\tilde{\ell} \to \ell\tilde{\chi}_2^0$ and $\tilde{\chi}_2^0 \to \tilde{\chi}_1^0\gamma$ must be taken into account. These cross-sections and branching ratios depend on the actual values of the SUSY parameters. The excluded regions for a given value of the common scalar mass, $\tilde{m}_0$, and $\tan\beta$ are presented in Figure(9) as a function of the Higgs superfield mass parameter μ and $\tilde{m}_{1/2}$.

9 Conclusions

In a data sample of 212 pb^{-1} collected by the DELPHI detector at centre-of-mass energies of 183 GeV and 189 GeV, searches were performed for events with acoplanar lepton pairs. The mass limits produced assume input parameters for the Higgs mass mixing parameter, μ, of -200 GeV/c^2 and ratio of the vacuum expectation value of the Higgs doublets, tanβ, of 1.5.

For the selectron pairs, 56 candidates remained after selection, with an expectation of 51.2 $\pm$ 1.5 from SM processes. This allowed a lower limit on the mass for the $\tilde{e}_R$ to be set at 87 GeV/c^2 for $\Delta m > 20$ GeV/c^2.

In the search for smuon production at 189 GeV, 17 events were selected for regions of low Δm, with 17.5 $\pm$ 0.3 expected from Standard Model processes. For regions of $\Delta m >$ 35 GeV/c^2, 7 candidates were selected, with a background expectation of 9.2 $\pm$ 0.2 events. At 183 GeV, 5 candidates were selected with a background expectation of 6.1 $\pm$ 0.6 events. Combining these data, a mass limit for $\tilde{\mu}_R$ of 80 GeV/c^2 was obtained for $\Delta m > 5$ GeV/c^2 .

In the search for stau production, 7 events were selected at 183 GeV with 7.5 $\pm$ 0.5 expected from SM processes. At 189 GeV, 9 candidates passed the selection criteria with a background of 10.6 $\pm$ 0.7 expected. Combining this data with all our previous data at lower energies[1], a mass limit for the stau can be set at 75 GeV/c^2 if the stau is purely a partner to the right handed tau, and at 73 GeV/c^2 if the stau mixing angle is such that the production cross-section is minimal.

In the search for a low-mass stau, 122 events were selected in the mass region below 15 GeV/c^2 and 50 events in the region between 15 GeV/c^2 and 27 GeV/c^2 . The background was 150.1 $\pm$ 2.3 and 55.7 $\pm$ 1.7 in the two regions. Combining these results with

all previous data [1], a $\tilde{\tau}$ with mass below 12.5 GeV/c^2 can be excluded for any mixing angle, provided that Δm is greater than m_τ.

Events with the topology of $e^+e^-\gamma\gamma$, $\mu^+\mu^-\gamma\gamma$, and missing energy were analysed and a search for $\tilde{\ell} \to \ell\tilde{\chi}_2^0 \to \ell\gamma\tilde{\chi}_1^0$ was performed. For the cascade decay selectron search 5 events were selected with an expectation of 4.2 $\pm$ 0.9 from SM process. For the smuon case 3 events remained with an expectation of 2.9 $\pm$ 0.7. No excess over the Standard Model prediction was found.

Acknowledgements

We are greatly indebted to our technical collaborators, to the members of the CERN-SL Division for the excellent performance of the LEP collider, and to the funding agencies for their support in building and operating the DELPHI detector.
We acknowledge in particular the support of
Austrian Federal Ministry of Science and Traffics, GZ 616.364/2-III/2a/98,
FNRS–FWO, Belgium,
FINEP, CNPq, CAPES, FUJB and FAPERJ, Brazil,
Czech Ministry of Industry and Trade, GA CR 202/96/0450 and GA AVCR A1010521,
Danish Natural Research Council,
Commission of the European Communities (DG XII),
Direction des Sciences de la Matière, CEA, France,
Bundesministerium für Bildung, Wissenschaft, Forschung und Technologie, Germany,
General Secretariat for Research and Technology, Greece,
National Science Foundation (NWO) and Foundation for Research on Matter (FOM), The Netherlands,
Norwegian Research Council,
State Committee for Scientific Research, Poland, 2P03B06015, 2P03B1116 and SPUB/P03/178/98,
JNICT–Junta Nacional de Investigação Científica e Tecnológica, Portugal,
Vedecka grantova agentura MS SR, Slovakia, Nr. 95/5195/134,
Ministry of Science and Technology of the Republic of Slovenia,
CICYT, Spain, AEN96–1661 and AEN96-1681,
The Swedish Natural Science Research Council,
Particle Physics and Astronomy Research Council, UK,
Department of Energy, USA, DE–FG02–94ER40817.

References

[1] DELPHI Collaboration, P. Abreu *et al.*, E. Phys. J. **C6** (1999) 385.

[2] ALEPH Collaboration, R. Barate *et al.*, Phys. Lett. **B469** (1999) 303.
L3 Collaboration, M. Acciari *et al.*, Phys. Lett. **B471** (1999) 280.
OPAL Collaboration, G. Abbiendi *et al.*, E. Phys. J. **C14** (2000) 51.

[3] P. Fayet and S. Ferrara, Phys. Rep. **32** (1977) 249.
H.P. Nilles, Phys. Rep. **110** (1984) 1.
H.E. Haber and G. L.Kane, Phys. Rep. **117** (1985) 75.

[4] H. Dreiner,"*Hide and Seek with Supersymmetry*", Zuoz Summer School on Hidden Symmetries and Higgs Phenomena, hep-ph/9902347, Switzerland, 1998.

[5] S. P. Martin, "*Perspectives on Supersymmetry*", Editor G .L. Kane, World Scientific, 1998.

[6] M. Drees, "*An Introduction to Supersymmetry*", hep-ph/9611409, 1996.

[7] DELPHI Collaboration, P. Aarnio *et al.*, Nucl. Instr. and Meth. **A303** (1991) 233.

[8] DELPHI Collaboration, P. Abreu *et al.*, Nucl. Instr. and Meth. **A378** (1996) 57.

[9] P. Chochula *et al.*, Nucl. Instr. and Meth. **A412** (1998) 304.

[10] T. Sjöstrand, Comp. Phys. Comm. **82** (1994) 74;
T. Sjöstrand, "*High energy physics event generation with* `PYTHIA 5.7` *and* `JETSET 7.4`", CERN TH/7111-93 (1993, rev. 1994).

[11] DELPHI Collaboration, P. Abreu *et al.*, Z. Phys. **C73** (1996) 11.

[12] S. Katsanevas and S. Melachroinos in '*Physics at LEP2*', CERN 96-01, Vol. 2, p. 328.

[13] F.A. Berends, R. Pittau and R. Kleiss, Comp. Phys. Comm. **85** (1995) 437.

[14] S. Jadach, B. F. L. Ward, and Z. Was, Comp. Phys. Comm **79** (1994) 503.

[15] F. A. Berends, R. Kleiss, and W. Hollik, Nucl. Phys. **B304** (1988) 712.
M. Böhm, A. Denner, and W. Hollik, Nucl. Phys. **B304** (1988) 687.

[16] S. Jadach, W. Placzek and B.F.L Ward, Phys. Lett. **B390** (1997) 298.

[17] T. Alderweireld *et al.*, CERN-OPEN-2000-141,
G. Altarelli *et al.*, (ed.) "Physics at LEP2", CERN 96-01, Vol II, p.224.

[18] F. A. Berends, P.H. Daverveldt and R. Kleiss, Comp. Phys. Comm. **40** (1986) 271.

[19] F. A. Berends, P.H. Daverveldt and R. Kleiss, Comp. Phys. Comm. **40** (1986) 285.

[20] K. Mönig, *"Model independent limit of the Z-decays Width into Unknown particles"*, CERN-OPEN-97-040.

[21] A. L. Read, *"Modified Frequentist Analysis of Search Results (The CLs Method)"*, CERN 2000-005, pp. 81-101.

$\sqrt{s}$ (GeV)	183	189
Observed events	11	45
Total background	12.7 ± 0.8	38.5 ± 1.3
$Z^0/\gamma \to (\mu\mu,ee,\tau\tau)(n\gamma)$	1.7 ± 0.2	1.4 ± 0.1
4-fermion events	10.5 ± 0.8	34.2 ± 1.3
$\gamma\gamma \to ee,\mu\mu,\tau\tau$	0.5 ± 0.1	2.9 ± 0.1

Table 1: Selectron candidates, together with the total number of background events expected and the contributions from major background sources. Results shown are for 54 pb^{-1} of data analysed at 183 GeVand 158 pb^{-1} of data analysed at 189 GeV.

	189 GeV		183 GeV
	$\Delta m \leq 35$ GeV/c^2	$\Delta m > 35$ GeV/c^2	All regions
Observed events	17	7	5
Total background	17.5 ± 0.3	9.2 ± 0.2	6.1 ± 0.6
$Z^0/\gamma \to (\mu\mu,ee,\tau\tau)(n\gamma)$	0.9 ± 0.1	1.6 ± 0.2	0.2 ± 0.1
4-fermion events	15.7 ± 0.3	5.5 ± 0.1	5.8 ± 0.6
$\gamma\gamma \to ee,\mu\mu,\tau\tau$	0.9 ± 0.1	2.1 ± 0.2	0.1 ± 0.1

Table 2: Smuon candidates, together with the total number of background events expected and the contributions from major background sources. The results are shown for the two regions of the SUSY mass space analysed at a centre-of-mass energy of 189 GeV, and the full mass spectrum analysed at a centre-of-mass energy of 183 GeV.

$\sqrt{s}$ (GeV)	183	189
Observed events	7	9
Total background	7.5 ± 0.5	10.6 ± 0.7
$Z^0/\gamma \to (\mu\mu,ee,\tau\tau,q\overline{q})(n\gamma)$	1.0 ± 0.3	1.5 ± 0.2
4-fermion events	5.0 ± 0.3	7.2 ± 0.4
$\gamma\gamma \to \tau^+\tau^-$	0.9 ± 0.2	0.8 ± 0.3
$\gamma\gamma \to ee,\mu\mu,\ q\overline{q}$	0.6 ± 0.1	1.1 ± 0.5

Table 3: Stau candidates in the search for high mass staus, together with the total number of background events expected and the contributions from major background sources for centre-of-mass energies of 183 GeVand 189 GeV.

	$m_{\tilde{\tau}} < 15$ GeV/c^2		15 GeV/$c^2 \leq m_{\tilde{\tau}} < 27$ GeV/c^2	
$\sqrt{s}$ (GeV)	183	189	183	189
Observed events	31	91	12	38
Total background	38.8 ± 1.5	111.3 ± 1.8	14.4 ± 0.9	41.3 ± 1.4
$Z^0/\gamma \to (\mu\mu, ee, \tau\tau, q\overline{q})(n\gamma)$	30.9 ± 1.4	86.5 ± 1.5	7.6 ± 0.7	19.9 ± 0.7
Bhabha	1.1 ± 0.2	3.3 ± 0.7	0.3 ± 0.1	0.9 ± 0.4
4-fermion events	3.9 ± 0.3	12.8 ± 0.5	3.9 ± 0.3	12.6 ± 0.4
$\gamma\gamma \to \tau^+\tau^-$, ee , $\mu\mu$, $q\overline{q}$	2.9 ± 0.4	8.7 ± 0.6	2.6 ± 0.4	7.9 ± 1.1

Table 4: Stau candidates in the search for low-mass staus, together with the total number of background events expected and the contributions from major background sources for centre-of-mass energies of 183 GeV and 189 GeV.

Observed events	5
Total background	4.2 ± 0.9
Bhabha	2.0 ± 0.4
$\gamma\gamma \to \tau^+\tau^-$	1.3 ± 0.7
$e^+e^- \to \tau^+\tau^-$	0.6 ± 0.3
4-fermion	0.3 ± 0.3

Table 5: Break down of the individual contributions to the tight $ee\gamma\gamma$ sample. Results presented are for data taken at centre-of-mass energies of 183 GeV and 189 GeV.

Observed events	3
Total background	2.9 ± 0.7
$e^+e^- \to \mu\mu$	0.9 ± 0.4
$e^+e^- \to \tau\tau$	1.2 ± 0.5
4-fermion events	0.8 ± 0.3

Table 6: Break down of the individual contributions to the tight $\mu\mu\gamma\gamma$ sample. Results presented are for data taken at centre-of-mass energies of 183 GeV and 189 GeV.

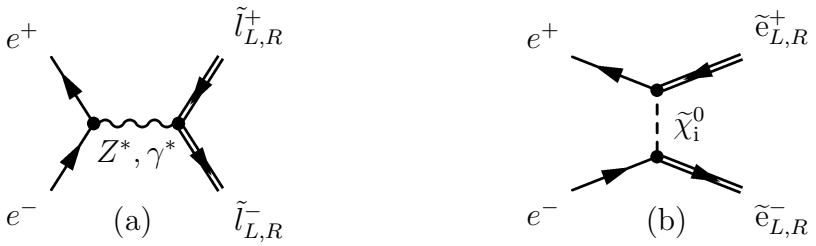

Figure 1: Production diagrams for sleptons in the MSSM. (a) Shows the pair-production of sleptons, a possible scenario at collider experiments. (b) Shows the additional t-channel contribution to selectron production.

Figure 2: Slepton decay diagrams. (a) Shows the slepton decaying into a lepton of same flavour and the LSP. (b) Shows the cascade decay; the slepton decaying into the lepton plus the second lightest neutralino, followed by a radiative decay to the LSP.

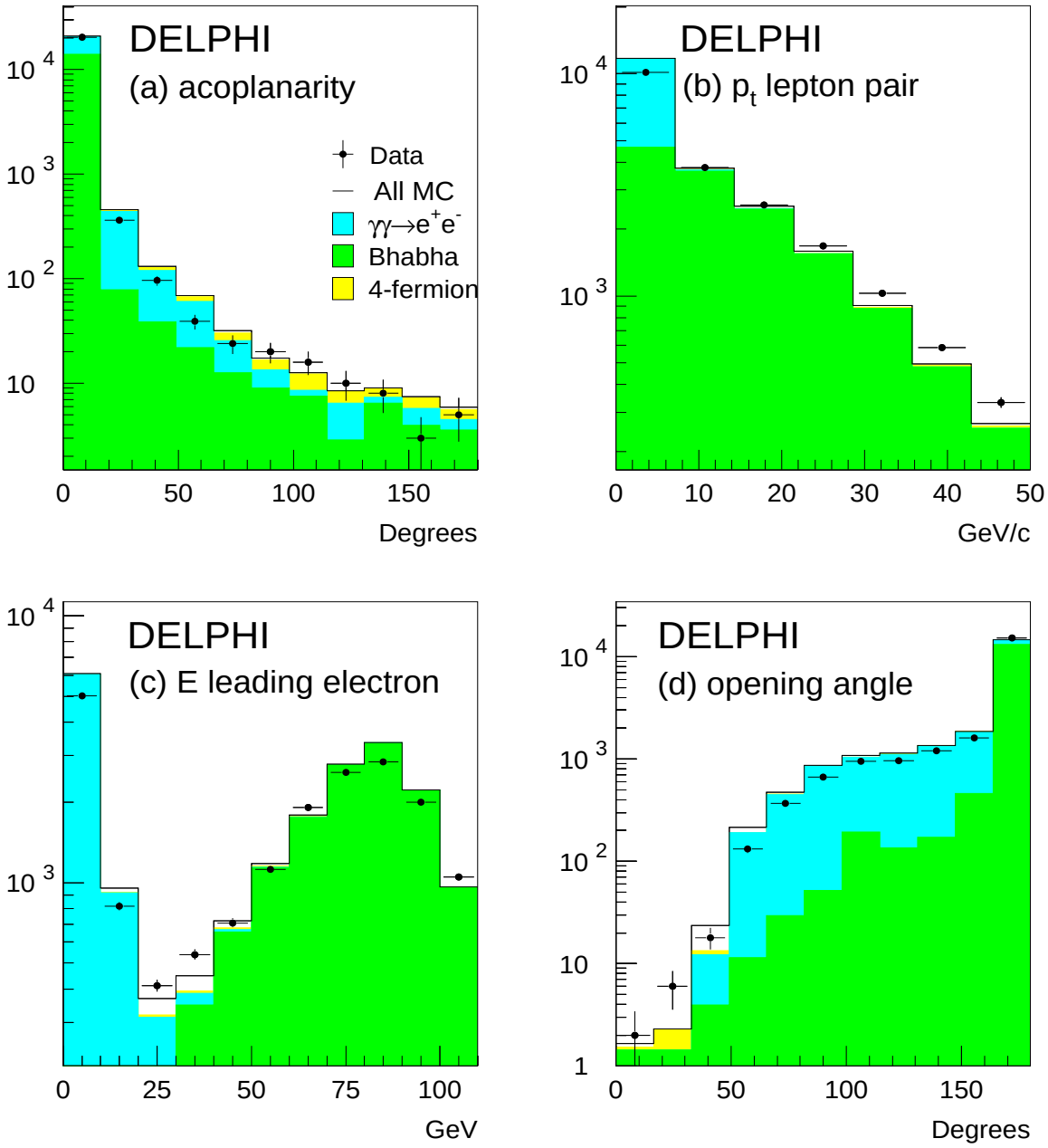

Figure 3: A pre-selection comparison of data and simulated SM events in the selectron analysis at 189 GeV. The plots show; (a) Electron pair acoplanarity, (b) Transverse momentum of the electron pair, (c) Energy of leading electron, (d) Opening angle between lepton pair. The dots with error bars show the data, while the simulation is plotted as a histogram.

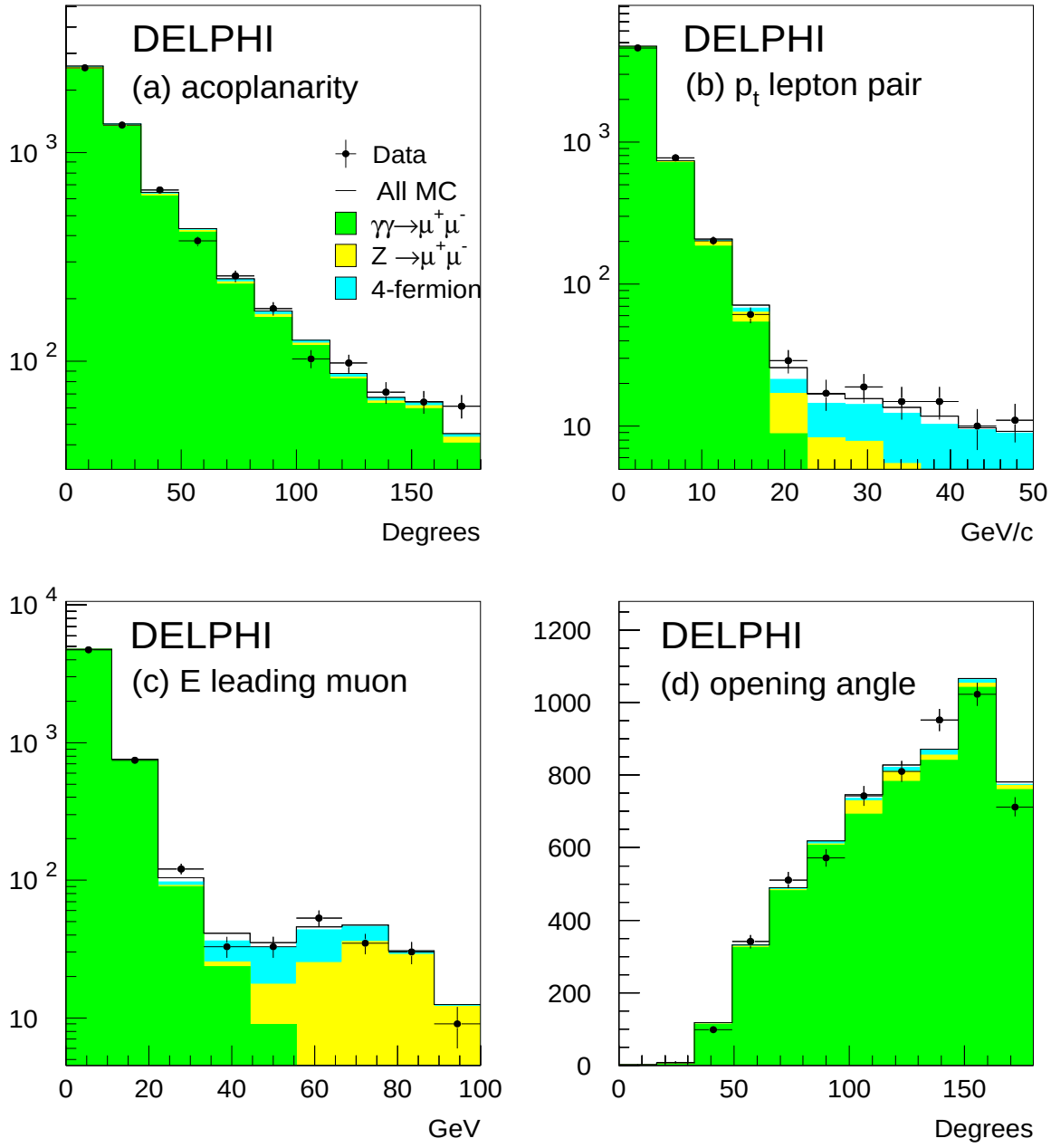

Figure 4: A pre-selection comparison of data and simulated SM events in the smuon analysis at 189 GeV. The plots show; (a) Muon pair acoplanarity (b) Transverse momentum of the muon pair, (c) Energy of leading muon, (d) Opening angle of the muon pair. The dots with error bars show the data, while the simulation is plotted as a histogram.

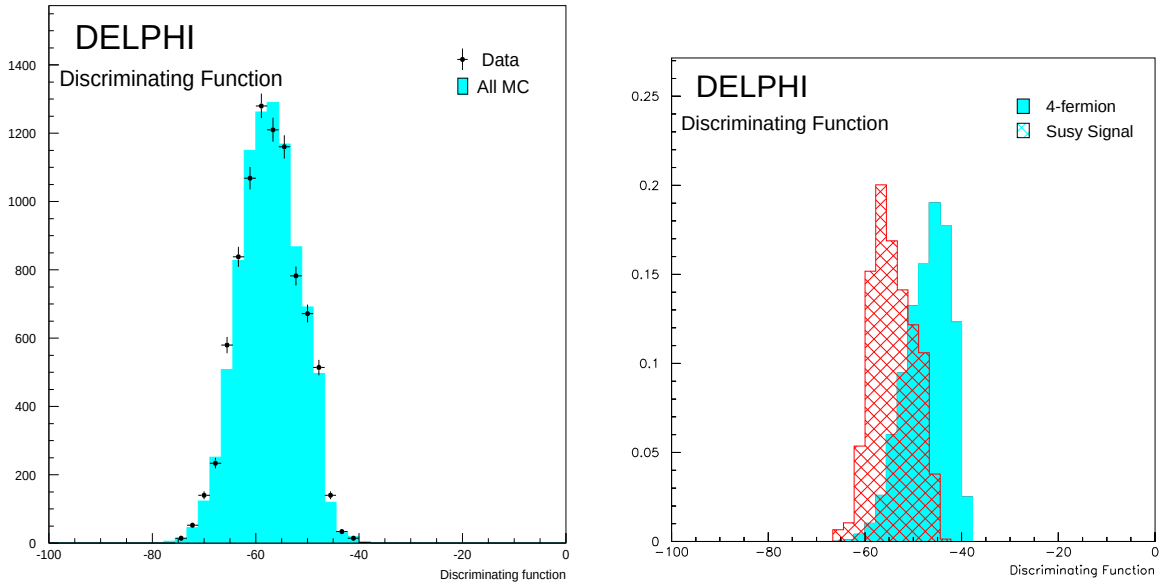

Figure 5: Function used to discriminate against W-pair backgrounds. Left: The points represent the data and the solid histogram shows the contribution from Standard Model backgrounds. Right: The discriminating function for a sample of 4-fermion events (solid) and SUSY signal events (hashed). Note: the right hand plot is shown for illustration purposes only.

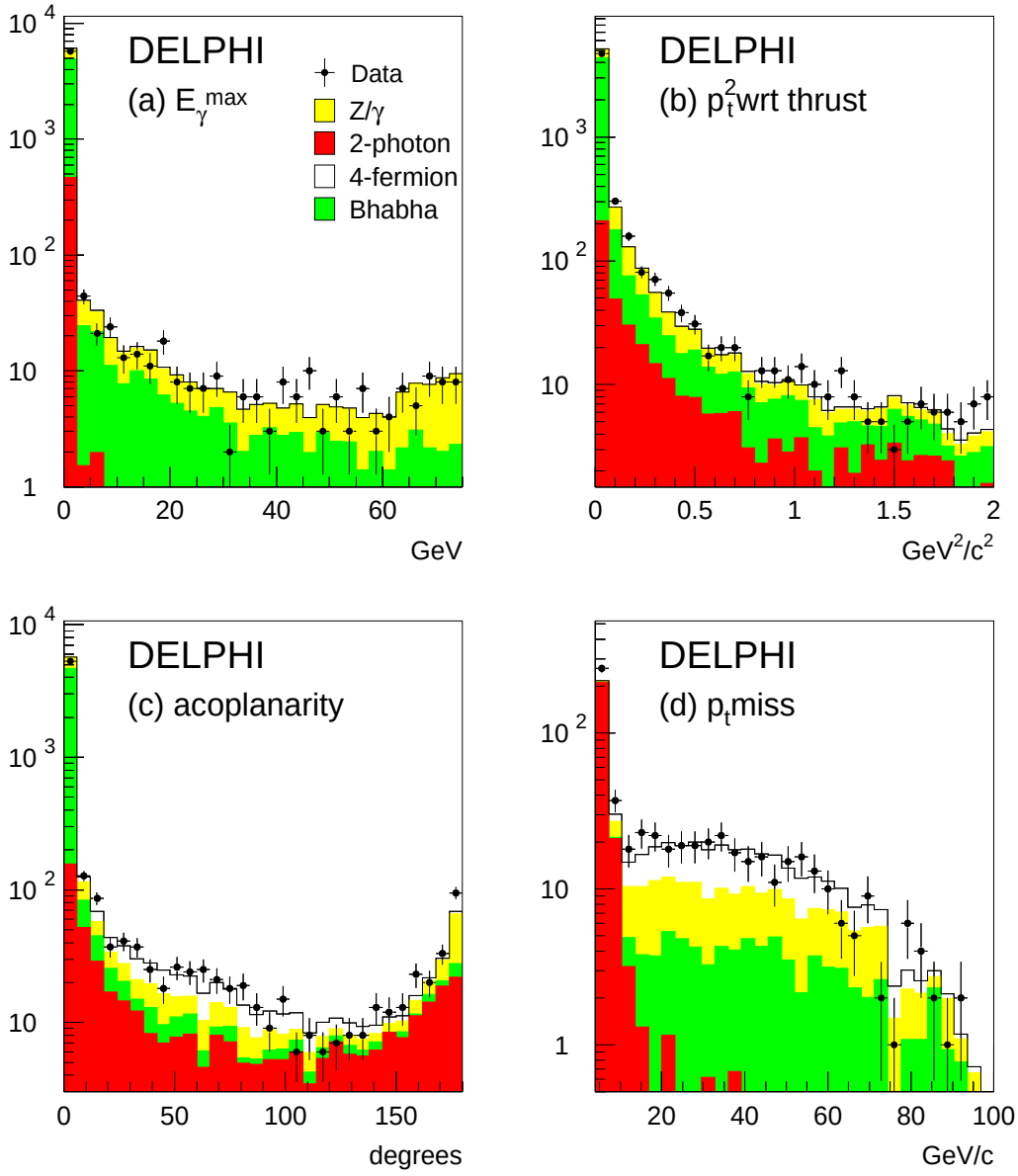

Figure 6: A pre-selection comparison of data and simulated SM events in the stau analysis at 189 GeV. The plots show: (a) Energy of the most energetic, isolated photon (b) The square of the transverse momentum with respect to the thrust axis (c) The acoplanarity (d) Missing transverse momentum, for events with acoplanarity above 10 degrees. The dots with error bars show the data, while the simulation is shown by the histogram.

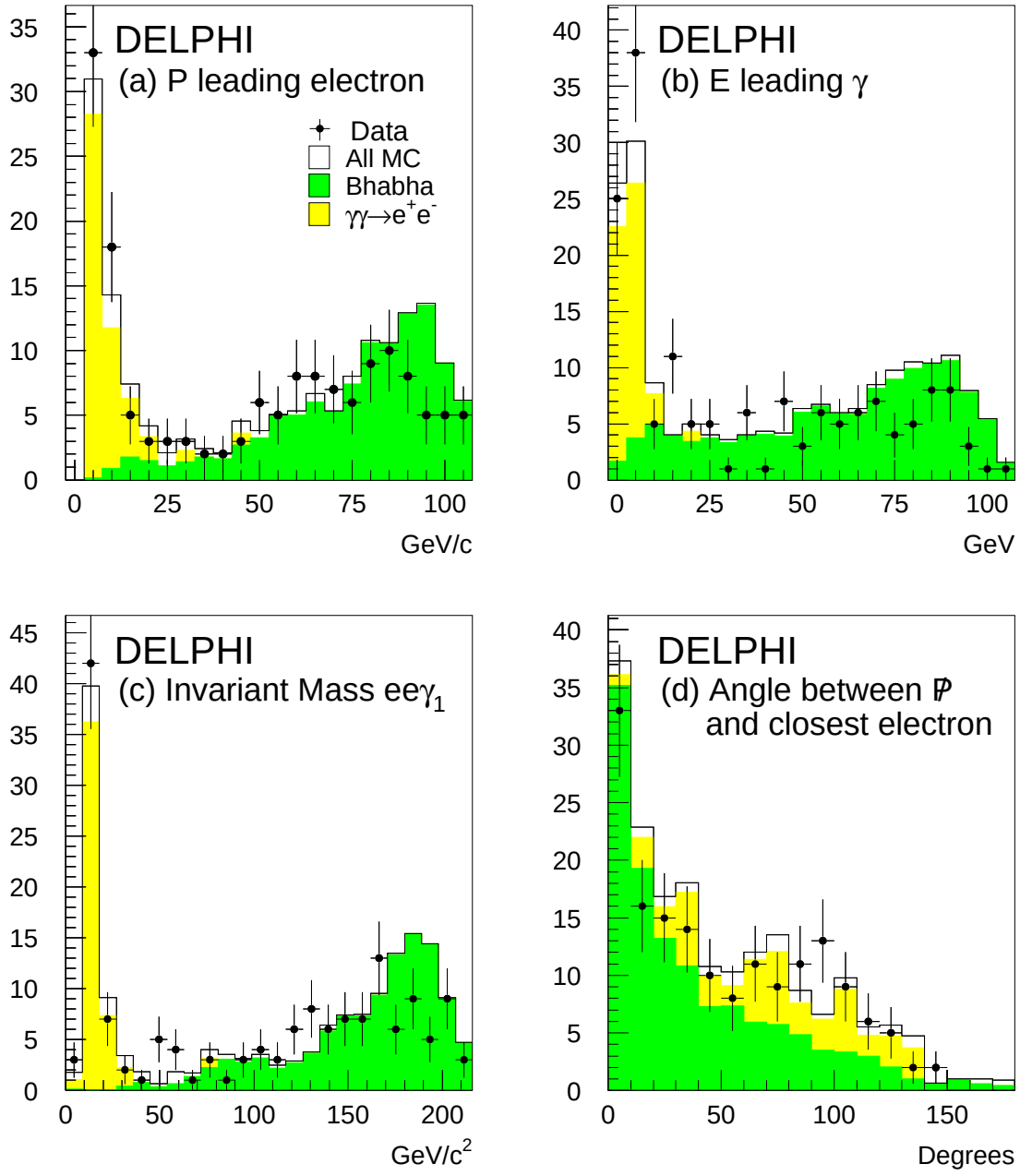

Figure 7: A pre-selection comparison of real data and simulated SM events in the electron channel of the cascade decay search. The plots show (a) Momentum of leading electron, (b) Energy of leading photon, (c) The invariant mass $M_{ee\gamma_1}$, (d) The angle between the missing momentum and the closest electron.

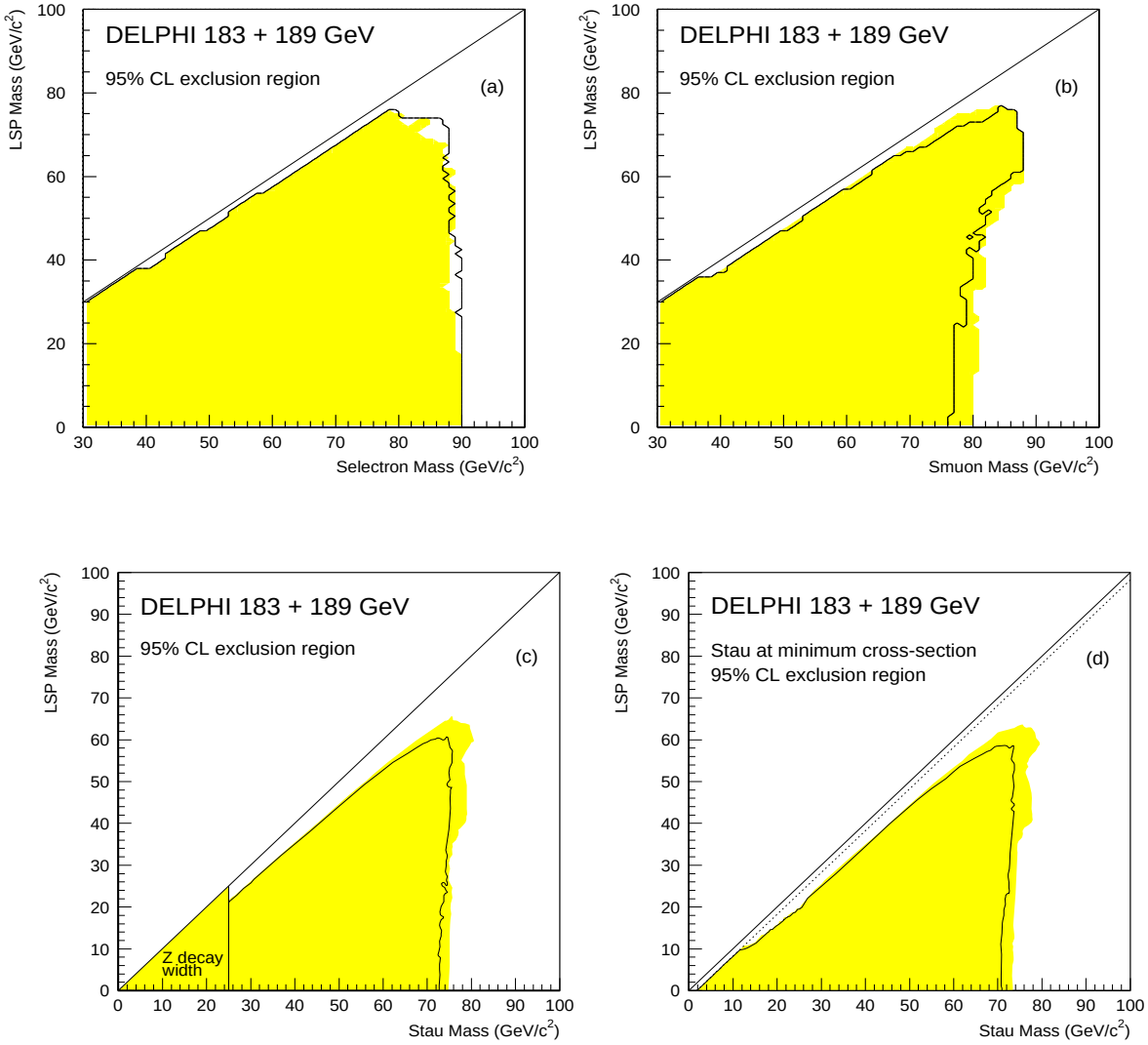

Figure 8: 95% CL exclusion regions for $\tilde{\ell}\tilde{\ell}$ production in the MSSM. Figures (a) and (b) show respectively the exclusion region for $\tilde{e}_R, \tilde{\mu}_R$ production in the $(\tilde{\ell},\tilde{\chi}_1^0)$ mass plane. Figures (c) and (d) show the mass exclusion regions for the $\tilde{\tau}_R$ and $\tilde{\tau}_{min}$ in the $(\tilde{\tau},\tilde{\chi}_1^0)$ mass plane. The shaded region in the plots shows the obtained exclusion limit, and the solid line shows the expected limit treating simulated background as data. In (d), the dotted line represents $\Delta m = m_\tau$. The limits have been produced using values of tanβ=1.5 and μ = -200 GeV/c^2.

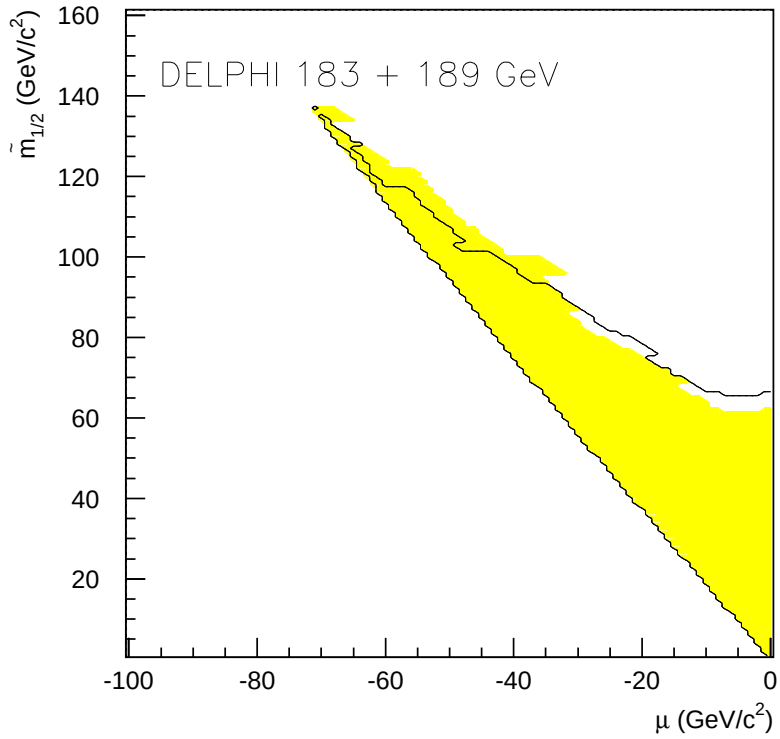

Figure 9: Exclusion regions at 95 % CL in the SUSY parameter space from the $\ell\ell\gamma\gamma$ events. The shaded region shows the obtained limit, and the solid line shows the limit treating simulated background as data. The exclusion region is obtained assuming a slepton mass ,$m_{\tilde{\ell}} = 80$ GeV/c^2, and a value of tan$\beta = 1.0$. The slepton mass of 80 GeV/c^2 was chosen as it was the highest excluded mass from the $\tilde{e}, \tilde{\mu}$ direct decay search.